Breakdown of the Fermi Liquid Description for Strongly Interacting Fermions

Yoav Sagi, Tara E. Drake, Rabin Paudel, Roman Chapurin, and Deborah S. Jin*
JILA, National Institute of Standards and Technology and the University of Colorado, and the Department of Physics, University of Colorado, Boulder, Colorado 80309-0440, USA
(Received 7 October 2014; published 19 February 2015)

The nature of the normal state of an ultracold Fermi gas in the BCS-BEC crossover regime is an intriguing and controversial topic. While the many-body ground state remains a condensate of paired fermions, the normal state must evolve from a Fermi liquid to a Bose gas of molecules as a function of the interaction strength. How this occurs is still largely unknown. We explore this question with measurements of the distribution of single-particle energies and momenta in a nearly homogeneous gas above T_c. The data fit well to a function that includes a narrow, positively dispersing peak that corresponds to quasiparticles and an "incoherent background" that can accommodate broad, asymmetric line shapes. We find that the quasiparticle's spectral weight vanishes abruptly as the strength of interactions is modified, which signals the breakdown of a Fermi liquid description. Such a sharp feature is surprising in a crossover.

DOI: 10.1103/PhysRevLett.114.075301 PACS numbers: 67.85.Lm, 03.75.Ss

Landau's Fermi liquid theory is a well-established and powerful paradigm for describing systems of interacting fermions [1,2]. It postulates that even in the presence of strong interactions, the system retains a Fermi surface and has low energy excitations that are long-lived, fermionic, and nearly noninteracting. The effect of interactions is incorporated into renormalized properties of these quasiparticle excitations, such as an effective mass, m^*, that is larger than the bare fermion mass, m, and a spectral weight, or quasiparticle residue, that is between zero and one [2]. While Fermi liquid theory is extremely successful in describing a wide range of materials, it fails in systems exhibiting strong fluctuations or spatial correlations. Understanding the origin of such breakdowns of a Fermi liquid description is an outstanding challenge in strongly correlated electron physics [3].

An ultracold Fermi gas with tunable interactions is a paradigmatic strongly correlated system. These atomic gases provide access to the crossover from Bardeen-Cooper-Schrieffer (BCS) superconductivity to Bose-Einstein condensation (BEC) of tightly bound fermion pairs [4–8]. The question of whether the Fermi liquid paradigm breaks down in the normal state of the crossover is related to the prediction of a "pseudogap" phase, where incoherent many-body pairing occurs above the transition temperature T_c. This pseudogap phase has bosonic (pair) excitations, in contrast to the fermionic excitations of a conventional Fermi liquid. In experiments that probed the strongly interacting gas in the middle of the crossover, Fermi-liquid-like behavior was observed in thermodynamics [9,10] and spin transport properties [11]. Meanwhile, evidence for pairing above T_c was reported in photoemission spectroscopy (PES) measurements [12], which reveal the distribution of single-particle energies and momenta in a many-body system [13,14]. Interpretation of these data has been controversial, with a Fermi liquid theory and a pseudogap theory, each separately argued to agree with the observations [15–17]. Issues raised include the fact that the PES measurements probed a trapped gas, where averaging over the inhomogeneous density can obscure the intrinsic physics [15,18], and that thermodynamics measurements are relatively insensitive to a pseudogap compared to spectroscopy. Thus, the question of how a Fermi liquid evolves into a Bose gas of paired fermions in the BCS-BEC crossover, and whether a Fermi liquid description breaks down, remains open. Here, we answer this question with the first PES of a nearly homogeneous Fermi gas; we perform measurements above T_c for a range of interaction strengths through the crossover [Fig. 1(a)], and find that quasiparticle excitations, which exist on the BCS side, vanish abruptly beyond a certain interaction strength on the BEC side.

We prepare a gas of ^{40}K atoms in an equal mixture of two spin states, where the scattering length, a, that parametrizes the interactions is varied using a Fano-Feshbach scattering resonance [22] [see Fig. 1(a) and Supplemental Material [23]]. To eliminate the complications arising from density inhomogeneity, we combine momentum-resolved rf spectroscopy [13] [Fig. 1(b)] with spatially selective imaging that probes only atoms from the trap center where the density is the highest and has the smallest spatial gradients [20] [Fig. 1(c)]. The lower panel of Fig. 1(d) shows PES data taken above T_c for several values of $(k_F a)^{-1}$, where k_F is the Fermi wave number. The PES signal, $I(k, E)$, is proportional to $k^2 A(k, E) f(E)$, where $A(k, E)$ is the atomic spectral function [13,30] and $f(E)$ is the Fermi function. Here, E and k are in units of E_F and k_F, respectively, and we normalize each data set so that the integral over all k and E equals 1.

The data in Fig. 1(d) show an evolution from a positively dispersing, quasiparticle-like spectrum to a broad, negatively

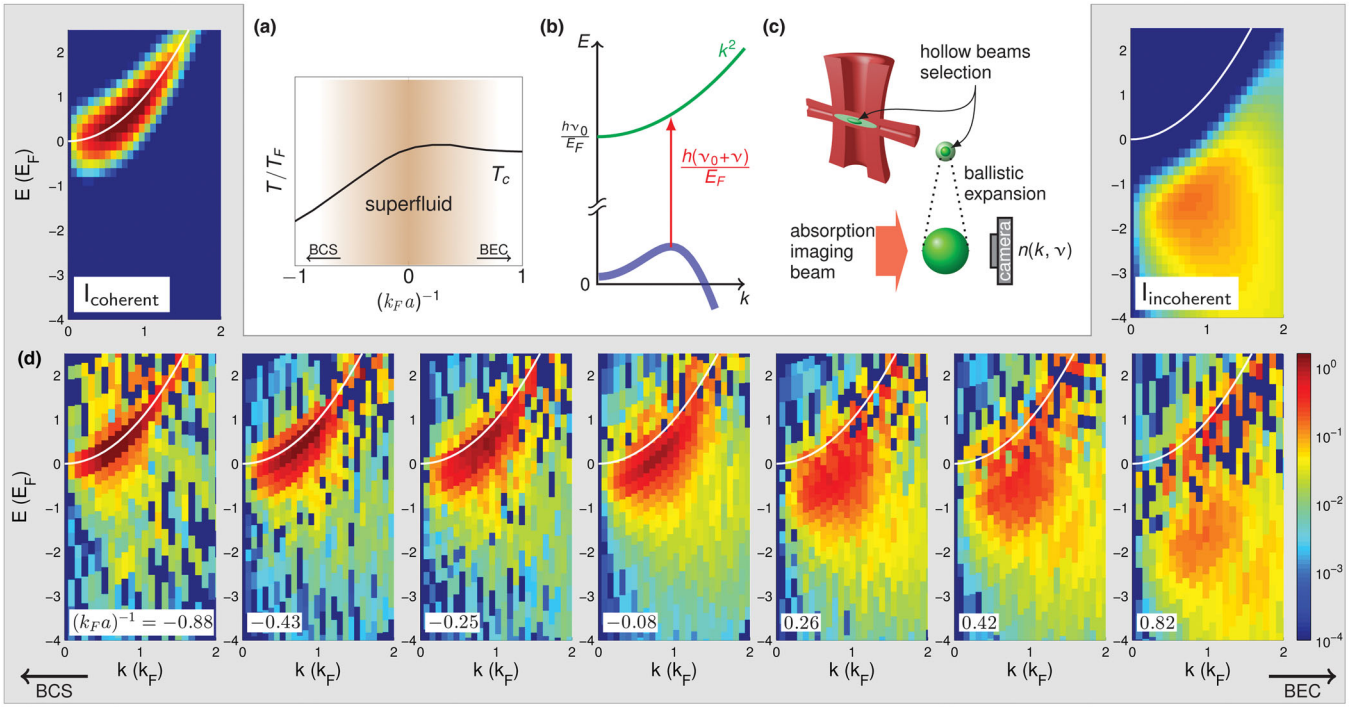

FIG. 1 (color). Atom PES data. (a) We take data above T_c in the strongly interacting region of the BCS-BEC crossover [19]. After initially preparing the gas at small, positive a, the magnetic field is swept adiabatically to a final value within the BCS-BEC crossover, where $|(k_F a)^{-1}| < 1$. (b) Schematically, a rf photon, which has a negligible momentum, transfers an atom from the strongly interacting state (blue line) to a weakly interacting state (green line). The energy and momentum of the atom in the strongly interacting state are extracted from the measured momentum of the spin-flipped atom and the rf detuning ν [13]. The detuning, ν, of the rf frequency is varied to obtain data for a wide range of E and k. (c) Immediately following the rf pulse and before time-of-flight expansion, two orthogonally propagating hollow-core beams optically pump atoms at the edges of the outcoupled atom cloud into a dark state [20,21]. The durations of both the rf pulse and optical pumping are short compared to the motion of atoms in the trap. (d) (lower panel) In these example plots of PES data, the color represents the probability distribution of atoms at a given E and k in the strongly interacting gas. We estimate that the error bar of $(k_F a)^{-1}$ is 0.03. $E = 0$ is the energy of a free atom at rest and the white line shows the free-particle dispersion $E = k^2$. (d) (upper panel) Our two-mode fit function includes a fermionic quasiparticle part, shown on the left with $m^* = 1.05$, $E_0 = -0.1$, $\mu = 0.5$, and $T = 0.25$, and an incoherent part, shown on the right with $E_p = 1.5$ and $T_p = 0.7$.

dispersing spectrum. Previous trap-averaged atom PES data showed back-bending and large energy widths [12,16]. These features are also apparent in the nearly homogeneous data [23]. However, these data are more amenable to quantitative analysis because k_F (and E_F) are approximately single-valued across the sample. Similar to the analysis done in electron systems, we use a two-mode function to describe the PES signal [31]

$$I(k, E) = Z I_{\text{coherent}}(k, E) + (1 - Z) I_{\text{incoherent}}(k, E), \quad (1)$$

where the first part describes quasiparticles with a positive dispersion, the second part accommodates an "incoherent background" that exhibits negative dispersion, and Z is the quasiparticle spectral weight. When these two parts (defined below) are combined, the resulting dispersion can exhibit back-bending.

The quasiparticles in Fermi liquid theory are long-lived and, therefore, give rise to narrow energy peaks, which, in principle, could be directly observed. However, such peaks would be broadened by our experimental resolution of about $0.25 E_F$. This resolution is set by the number of atoms (with E_F scaling only weakly with increasing N) and the rf pulse duration (see Supplemental Material [23]), which must be short compared to the harmonic trap period in order to probe momentum states. We convolve Eq. (1) with a Gaussian function that accounts for our energy resolution before fitting to the data in order to determine the spectral weight of the quasiparticles [Fig. 1(d), upper panel].

To describe quasiparticles, we use

$$I_{\text{coherent}}(k, E) = 4\pi k^2 \delta\left(E - \frac{k^2}{m^*} - E_0\right) \times \frac{\{-(\pi m^* T)^{3/2} \text{Li}_{3/2}[-\exp(\frac{-E_0+\mu}{T})]\}^{-1}}{\exp(\frac{E-\mu}{T}) + 1}, \quad (2)$$

which consists of a quadratic dispersion of sharp quasiparticles multiplied by a normalized Fermi distribution (δ is

the Dirac delta function, and Li is the polylogarithm function). We include, as fit parameters, a Hartree shift E_0, effective mass m^*, chemical potential μ, and temperature T. Here, energies are given in units of E_F and m^* in units of m. This description of Fermi liquid quasiparticles is typically only used very near k_F and for T approaching zero, whereas we fit to data for a larger range in k and with temperatures near $0.2\ T_F$ (just above T_c). The latter is necessitated by the unusually large interaction energy compared to E_F, and we note that $0.2\ T_F$ is still sufficiently cold that one can observe a sharp Fermi surface in momentum [20]. Any increase in quasiparticle widths away from k_F will have little effect on the data as long as the quasiparticles have an energy width less than our energy resolution, which should be the case for long-lived quasiparticles. Finally, using a quadratic dispersion over a large range of k is supported by the data [23].

The second part of Eq. (1) needs to accommodate the remainder of the signal, which is often referred to as an "incoherent background" in a Fermi liquid description. For fermions with contact interactions, one expects an incoherent background at high momentum due to short-range pair correlations [32–34]. Motivated by this and by the normal state in the BEC limit, we use for $I_{\text{incoherent}}$ a function that describes a thermal gas of pairs. The pairs have a wave function that decays as $\exp(-r/R)$, where r is the relative distance and R is the pair size [35], and a Gaussian distribution of center-of-mass kinetic energies characterized by an effective temperature T_p. This gives

$$I_{\text{incoherent}}(k,E) = \Theta(-E_p - E + k^2) \times \frac{8k\sqrt{\frac{E_p}{T_p}}\exp^{\frac{E_p+E-3k^2}{T_p}}\sinh\left(\frac{2\sqrt{2}k\sqrt{-E_p-E+k^2}}{T_p}\right)}{\pi^{3/2}(E-k^2)^2}, \quad (3)$$

where Θ is the Heaviside step function, E_p is a pairing energy defined by $k_F R = \sqrt{2/E_p}$, and both E_p and T_p are dimensionless fitting parameters (see Supplemental Material [23]). While this description of the incoherent piece may not fully capture the microscopic behavior except in the BEC limit, we find, nonetheless, that Eq. (1), after convolution with a Gaussian that accounts for our energy resolution, fits the data very well throughout the crossover. For each value of $(k_F a)^{-1}$, we perform a surface fit to the roughly 300 points that comprise the PES data $I(k,E)$ for $k \leq 1.5$ and $E \geq -3$. The reduced chi-squared statistic, χ^2, after accounting for the seven fit parameters, is between 0.75 and 1.3. An example fit is shown in Fig. 2, where we show several traces at fixed k for PES data taken near unitarity.

In Fig. 3(a), we show Z as a function of $(k_F a)^{-1}$. For our lowest $(k_F a)^{-1}$, $Z \approx 0.8$; however, Z decreases rapidly going from the BCS side of the crossover (negative a) to the BEC side (positive a), reaching $Z \approx 0.3$ at unitarity. Beyond $(k_F a)^{-1} = 0.28 \pm 0.02$, Z vanishes, signalling the breakdown of a Fermi liquid description. Restricting the fitting to a smaller region around k_F gives results for Z that are consistent with the fits to $k \leq 1.5$ [see Fig. 3(a)]. We note that the interaction strength where Z vanishes, as well as the sharpness with which Z goes to zero, are likely to be temperature dependent [36]. The best fit values for the effective mass, m^* are shown in Fig. 3(b), where m^* increases with increasing interaction strength as expected for a Fermi liquid. A linear fit gives $m^* = 1.21 \pm 0.03$ at unitarity, which is somewhat higher than $m^* = 1.13 \pm 0.03$ measured in Ref. [9], but close to the $T = 0$ prediction of $m^* = 1.19$ from Ref. [18]. The other fit parameters for the two-mode function are shown in Fig. S4 in Ref. [23].

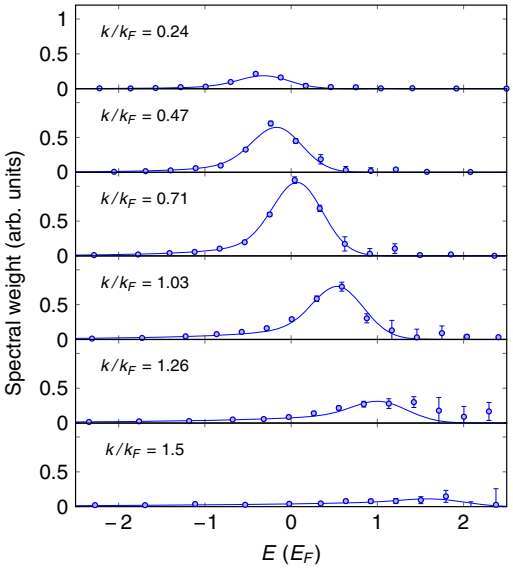

FIG. 2 (color online). EDCs for atom PES data near unitarity. Data (circles) and fits (lines) are shown for several example traces at fixed k through the PES data at $(k_F a)^{-1} = -0.08$. These traces are often called energy distribution curves, or EDCs. Here, the fitting parameters are $Z = 0.37 \pm 0.03$, $m^* = 1.22 \pm 0.03$, $T = 0.24 \pm 0.02$, $E_0 = -0.33 \pm 0.02$, $\mu = 0.19 \pm 0.04$, $E_p = 0.23 \pm 0.04$, $T_p = 1.09 \pm 0.08$, where the error margins are for one standard deviation and also include a 5% uncertainty in E_F. For this fit, the reduced χ^2 is 1.2.

We note an interesting comparison of our results with the Fermi polaron, which is the quasiparticle in the limit of a highly imbalanced Fermi gas. Schirotzek *et al.* measured $Z = 0.39 \pm 0.09$ for the Fermi polaron at unitarity [38], which is similar to our result for the balanced Fermi gas. For the polaron case, Z also goes to zero in a similar fashion to our results, but farther on the BEC side of the crossover [38]. This similarity is surprising because we expect a phase transition from polarons to molecules in the extreme imbalance limit [39,40], with Z acting as an order parameter [41], while, in contrast, the balanced Fermi gas should exhibit a continuous crossover. For m^*, we also find that

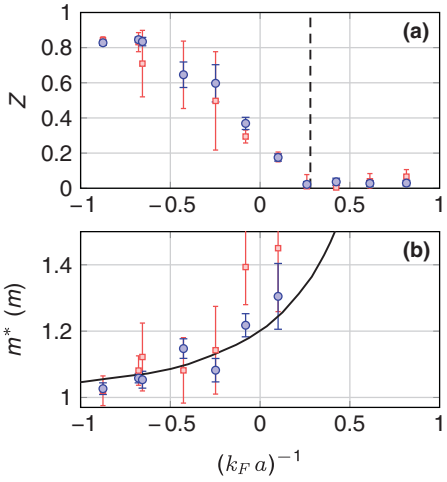

FIG. 3 (color). Z and effective mass. (a) The quasiparticle spectral weight Z decreases as $(k_F a)^{-1}$ increases. Using a linear fit to the range $-0.5 \leq (k_F a)^{-1} \leq 0.3$, we find that Z vanishes at $(k_F a)^{-1} = 0.28 \pm 0.02$ (dashed line); this marks the breakdown of a Fermi liquid description. The blue circles come from fits of a large range of data, from 0 to 1.5 k_F. The red squares show the result of restricting the fit to 0.7 to 1.3 k_F, and they show a similar trend and slightly larger error bars. (b) The quasiparticle effective mass m^* is shown for the region where $Z > 0$. Interactions increase m^*, and the data (circles) agree surprisingly well with the theoretical prediction for the limiting case of the Fermi polaron (solid line) [10,37]. Restricting the fit to EDCs close to the Fermi surface produces similar results with increased error bars (red squares).

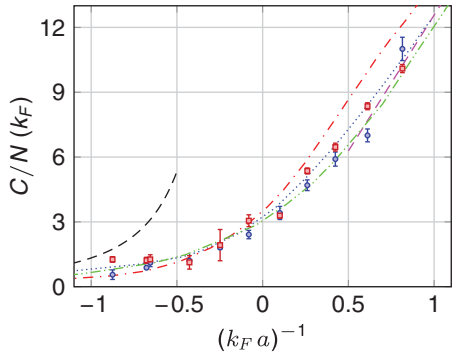

FIG. 4 (color). The contact parameter. From the PES data, we extract the contact per particle (in units of k_F) for a homogeneous Fermi gas above T_c as a function of the interaction strength $(k_F a)^{-1}$. The contact measured from the tail of the rf line shape [23], using data for $h\nu \geq 5E_F$, is shown in blue circles, while the contact extrapolated from the fits of the PES data is shown in red squares. Remarkably, even though we limited the fits of the PES data to $k \leq 1.5$ and $E \geq -3$, a region with a relatively small contribution of short-range correlations [21,32,33,42], we find that the contact from the PES fits is consistent with the contact measured from the tail of the momentum-integrated rf line shape. For comparison with the data, we also plot the BCS (dashed black line) and BEC (dashed magenta line) limits, given by $4(k_F a)^2/3$ and $4\pi(k_F a)^{-1}$, respectively [33], the non-self-consistent t-matrix at $T = 0$ (dotted blue line) and its Popov version at T_c (dashed-dotted red line) [44], and the self-consistent t-matrix model at $T = 0$ (double-dotted green line) [18]. Interestingly, we find that the contact measured above T_c agrees well with the $T = 0$ theories.

our result is close to the measured effective mass of the Fermi polaron at unitarity [9], $m^* = 1.20 \pm 0.02$, and similar to the predicted polaron mass [10,37] throughout our measurement range [solid line in Fig. 3(b)].

As $(k_F a)^{-1}$ increases, short-range correlations are expected to increase. This gives rise to increased weight in the high-k part of the spectral function [34], which is quantified by a parameter called the contact [21,32,33,42]. In a Fermi liquid description, the contact must be accounted for by the incoherent part of the spectral function [34]. We note that our particular choice for $I_{\text{incoherent}}$ has the expected form of a $1/k^4$ high-k tail in the momentum distribution [32] and a $1/\nu^{3/2}$ large-ν tail in the rf line shape [33], where ν is the rf detuning. Remarkably, we find that the contact can be accurately extracted from the fits to the PES data even though we restrict the fits to $k \leq 1.5$. For comparison, $1/k^4$ behavior in the momentum distribution was observed for $k > 1.5k_F$ [42]. In Fig. 4, we plot the measured contact per particle, C/N, in units of k_F, as a function of $(k_F a)^{-1}$. The data extend previous measurements of the contact at unitarity [18,44].

The results presented here can explain how different observations lead to different conclusions regarding the nature of the normal state of the unitary Fermi gas. Although the data here taken just above T_c show that a Fermi liquid description breaks down for $(k_F a)^{-1} \geq 0.28 \pm 0.02$, Z remains finite at unitary. Fermionic quasiparticles may play a key role in thermodynamics, while PES data reveal back-bending and significant spectral weight in an "incoherent" part that is consistent with pairing. With the nearly homogeneous PES data, we find that Z vanishes surprisingly abruptly and note some similarity to Fermi polaron measurements. Comparing the PES data with various BCS-BEC crossover theories may help elucidate these observations and advance quantitative understanding of the crossover.

This work was supported by the National Science Foundation under Grant No. 1125844 and by the National Institute of Standards and Technology. Y. S. and T. E. D. contributed equally to this work.

*Corresponding author.
jin@jilau1.colorado.edu.

[1] L. D. Landau, Sov. Phys. JETP **3**, 920 (1957).
[2] E. Lifshitz and L. P. Pitaevskii, *Statistical Physics, Part 2*, Landau and Lifshitz Course of Theoretical Physics Vol. 9 (Butterworth-Heinemann, Washington, DC, 1980).

[3] R. W. Hill, C. Proust, L. Taillefer, P. Fournier, and R. L. Greene, Nature (London) **414**, 711 (2001).
[4] C. A. Regal and D. S. Jin, Adv. At. Mol. Opt. Phys. **54**, 1 (2006).
[5] W. Ketterle and M. W. Zwierlein, in *Proceedings of the International School of Physics "Enrico Fermi", Course CLXIV*, edited by M. Inguscio, W. Ketterle, and C. Salomon (IOS Press, Amsterdam, 2008).
[6] Q. Chen, J. Stajic, S. Tan, and K. Levin, Phys. Rep. **412**, 1 (2005).
[7] W. Zwerger, *The BCS-BEC Crossover and the Unitary Fermi Gas*, Lecture Notes in Physics Vol. XVI (Springer, New York, 2012), p. 532.
[8] M. Randeria and E. Taylor, Annu. Rev. Condens. Matter Phys. **5**, 209 (2014).
[9] S. Nascimbène, N. Navon, K. J. Jiang, F. Chevy, and C. Salomon, Nature (London) **463**, 1057 (2010).
[10] N. Navon, S. Nascimbène, F. Chevy, and C. Salomon, Science **328**, 729 (2010).
[11] A. Sommer, M. Ku, G. Roati, and M. W. Zwierlein, Nature (London) **472**, 201 (2011).
[12] J. P. Gaebler, J. T. Stewart, T. E. Drake, D. S. Jin, A. Perali, P. Pieri, and G. C. Strinati, Nat. Phys. **6**, 569 (2010).
[13] J. T. Stewart, J. P. Gaebler, and D. S. Jin, Nature (London) **454**, 744 (2008).
[14] Q. Chen, Y. He, C.-C. Chien, and K. Levin, Rep. Prog. Phys. **72**, 122501 (2009).
[15] S. Nascimbène, N. Navon, S. Pilati, F. Chevy, S. Giorgini, A. Georges, and C. Salomon, Phys. Rev. Lett. **106**, 215303 (2011).
[16] A. Perali, F. Palestini, P. Pieri, G. C. Strinati, J. T. Stewart, J. P. Gaebler, T. E. Drake, and D. S. Jin, Phys. Rev. Lett. **106**, 060402 (2011).
[17] D. Wulin, H. Guo, C.-C. Chien, and K. Levin, Phys. Rev. A **83**, 061601 (2011).
[18] R. Haussmann, M. Punk, and W. Zwerger, Phys. Rev. A **80**, 063612 (2009).
[19] C. A. R. Sá de Melo, M. Randeria, and J. R. Engelbrecht, Phys. Rev. Lett. **71**, 3202 (1993).
[20] T. E. Drake, Y. Sagi, R. Paudel, J. T. Stewart, J. P. Gaebler, and D. S. Jin, Phys. Rev. A **86**, 031601 (2012).
[21] Y. Sagi, T. E. Drake, R. Paudel, and D. S. Jin, Phys. Rev. Lett. **109**, 220402 (2012).
[22] C. Chin, R. Grimm, P. Julienne, and E. Tiesinga, Rev. Mod. Phys. **82**, 1225 (2010).
[23] See Supplemental Material at http://link.aps.org/supplemental/10.1103/PhysRevLett.114.075301 for more information regarding methods, comparison to previous data, the form of the quasiparticle dispersion, derivation of the spectral function for pairs, additional fitting parameters, and extracting the contact, which includes Refs. [24–29].
[24] C. A. Regal, M. Greiner, and D. S. Jin, Phys. Rev. Lett. **92**, 040403 (2004).
[25] C. Regal, Ph.D. thesis, University of Colorado, 2006.
[26] P. Magierski, G. Wlazłowski, A. Bulgac, and J. E. Drut, Phys. Rev. Lett. **103**, 210403 (2009).
[27] J. J. Kinnunen, Phys. Rev. A **85**, 012701 (2012).
[28] G. M. Bruun and G. Baym, Phys. Rev. A **74**, 033623 (2006).
[29] E. Braaten, D. Kang, and L. Platter, Phys. Rev. A **78**, 053606 (2008).
[30] M. Veillette, E. G. Moon, A. Lamacraft, L. Radzihovsky, S. Sachdev, and D. E. Sheehy, Phys. Rev. A **78**, 033614 (2008).
[31] A. Damascelli, Z. Hussain, and Z.-X. Shen, Rev. Mod. Phys. **75**, 473 (2003).
[32] S. Tan, Ann. Phys. (Amsterdam) **323**, 2971 (2008).
[33] E. Braaten, in *The BCS-BEC Crossover and the Unitary Fermi Gas*, Lecture Notes in Physics, edited by W. Zwerger (Springer, Berlin, 2012), Vol. 836, pp. 193–231.
[34] W. Schneider and M. Randeria, Phys. Rev. A **81**, 021601 (2010).
[35] C. Chin and P. S. Julienne, Phys. Rev. A **71**, 012713 (2005).
[36] E. V. H. Doggen and J. J. Kinnunen, arXiv:1411.7207.
[37] R. Combescot, S. Giraud, and X. Leyronas, Europhys. Lett. **88**, 60007 (2009).
[38] A. Schirotzek, C.-H. Wu, A. Sommer, and M. W. Zwierlein, Phys. Rev. Lett. **102**, 230402 (2009).
[39] N. Prokof'ev and B. Svistunov, Phys. Rev. B **77**, 020408 (2008).
[40] N. V. Prokof'ev and B. V. Svistunov, Phys. Rev. B **77**, 125101 (2008).
[41] M. Punk, P. T. Dumitrescu, and W. Zwerger, Phys. Rev. A **80**, 053605 (2009).
[42] J. T. Stewart, J. P. Gaebler, T. E. Drake, and D. S. Jin, Phys. Rev. Lett. **104**, 235301 (2010).
[43] E. D. Kuhnle, S. Hoinka, P. Dyke, H. Hu, P. Hannaford, and C. J. Vale, Phys. Rev. Lett. **106**, 170402 (2011).
[44] F. Palestini, A. Perali, P. Pieri, and G. C. Strinati, Phys. Rev. A **82**, 021605 (2010).